Angle-Resolved Second-Harmonic Light Scattering from Colloidal Particles

N. Yang, W. E. Angerer, and A. G. Yodh

Department of Physics and Astronomy, University of Pennsylvania, 209 South 33rd Street, Philadelphia, Pennsylvania 19104-6396

(Received 16 March 2001; published 16 August 2001)

We report angle-resolved second-harmonic generation (SHG) measurements from suspensions of centrosymmetric micron-size polystyrene spheres with surface-adsorbed dye (malachite green). The second-harmonic scattering profiles differ qualitatively from linear light scattering profiles of the same particles. We investigated these radiation patterns using several polarization configurations and particle diameters. We introduce a simple Rayleigh-Gans-Debye model to account for the SHG scattering anisotropy. The model compares favorably with our experimental data. Our measurements suggest scattering anisotropy may be used to isolate particle nonlinear optics from other bulk nonlinear optical effects in suspension.

DOI: 10.1103/PhysRevLett.87.103902 PACS numbers: 42.65.–k, 33.80.–b, 78.70.–g, 78.68.+m

Linear light scattering from micron-size spherical particles was well understood during the past century [1,2], and currently provides the basis for characterization of a wide variety of particle dispersions ranging from colloids and emulsions to sprays, polymer solutions, and granular materials. By contrast, with a few notable exceptions [3,4], the nonlinear optical properties of particles were rarely investigated, in part because the theory is more complex, and in part because nonlinear scattering signals are small.

This situation has changed recently as a result of observations of second-harmonic generation (SHG) from centrosymmetric colloidal suspensions [5,6]. These observations have stimulated fundamental theoretical developments [7] and more experimentation [8–14]. Researchers are anticipating that the spectacular success of second-order nonlinear optical probes in surface and interface science [15,16] might be duplicated in studies of colloidal particle surfaces and related phenomena. In particular, an improved understanding of the chemical dynamics on particle surfaces may lead to better control of colloidal assembly, aggregation, and particle interactions.

In this Letter we present the first experimental measurements of SH angular radiation patterns due to colloids. Our experiments employ suspensions of $\sim$1-μm-diameter polystyrene spheres in aqueous solutions containing malachite green dye. Some of the dissolved malachite green preferentially adsorbs onto the particle surfaces, producing a large second-order surface nonlinearity which facilitates SHG when the particle is illuminated by light in the near-infrared [6]. Strong SHG is achieved because the emission of molecular radiators pointing in opposite directions on opposing surfaces of the particle does not interfere destructively; the finite size of the particle inhibits phase cancellation [7]. We measured the angle-resolved SH light scattering patterns in the standard polarization configurations for particles with different diameters. Our observations reveal qualitative differences between linear and nonlinear particle light scattering, notably the absence of forward scattering in the latter case and the presence of interesting secondary peaks. Some of these features are predicted by rigorous theory for Rayleigh particles [7]. We show, however, that it is possible to account for our data by using a simple nonlinear analog of Rayleigh-Gans-Debye (RGD) theory to describe the SHG scattering anisotropy of larger, e.g., Mie, particles. The anisotropic SHG scattering patterns may be used to differentiate bulk nonlinear optical effects from signals originating on the particle surfaces, and also as a basis for more quantitative predictions about molecules on particle surfaces.

Experiments were performed using a 76 MHz pulse train of ultrashort light pulses derived from a mode-locked Ti:Al_2O_3 laser operating at 840 nm. The apparatus is sketched in Fig. 1. Briefly, the Ti:Al_2O_3 output pulses had a temporal width of $\sim$100 fs and a peak power of $\sim$50 kW. The spatial profile of the beam was approximately Gaussian. The fundamental beam was passed through spectral filters to eliminate background photons at 2ω, and then

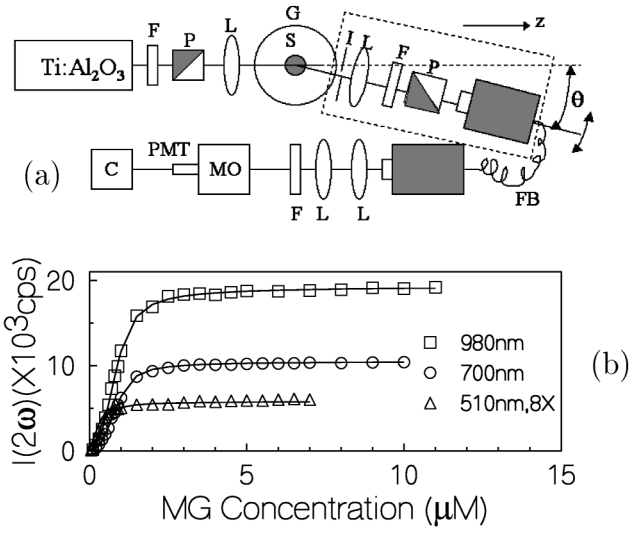

FIG. 1. (a) Experimental setup for SHG angular scattering measurement. F: spectral filter; P: polarizer; L: lens; G: goniometer; S: sample; I: iris; FB: fiber; MO: monochromator; PMT: photomultiplier tube; C: photon counter. The *s*-polarized (*p*-polarized) direction is perpendicular (parallel) to the paper plane. (b) Adsorption isotherms for MG on PS particles. The solid lines are fits to a modified Langmuir model.

focused into the sample cell; the beam waist at sample center was ~40 μm. The input beam polarization was set using a standard prism combination and polarizer [17]. A scattered signal at 2ω was recollimated, polarization selected, and then coupled into an optical fiber. The fiber output was recollimated, spectrally filtered, coupled into a monochromator for further spectral discrimination, and then directed onto a photomultiplier tube (PMT) detector. A lock-in photon counter was used for signal averaging. The background was below 1 count per second.

The most unique feature of our apparatus was its angular resolution. The sample was located at the center of a goniometer so that the entire detection arm could be rotated about the axis through the sample center and perpendicular to the scattering plane, facilitating angle-resolved scans. A low numerical aperture (0.16) detection fiber and a 1-mm-diameter iris determined our angular resolution of 1°.

Samples consisted of polystyrene (PS) spheres in water with diameters 0.51, 0.70, and 0.98 μm. The particle surfaces were negatively charged, with $-COO^-$ surface functional groups. Malachite green (MG) dye was mixed into the suspensions at varying concentrations. The amount of MG adsorbed on the PS particles was a function of MG concentration. Solution pH was fixed at ~5.7 [18] to preserve the dominant MG^+ form, and all measurements were performed at room temperature. Conventional dynamic light scattering experiments with the same laser system confirmed particle size and confirmed that the particles did not aggregate in suspension.

Figure 1(b) shows a set of adsorption isotherms for MG on PS. The results and experimental conditions are similar to those of Refs. [10,13]. For our angular profile measurements, we set the MG concentration to 7 μM and the particle density to 6.3×10^8 cm^{-3}. At these concentrations, the particle surfaces are saturated with MG, and the number density of MG molecules in the solution was ~10 times larger than the total number density of MG molecules on the particle surfaces. Therefore the solvent MG concentration was relatively insensitive to small changes in particle number.

In Fig. 2 we exhibit unprocessed angle-resolved suspension data, along with data from pure MG solutions at similar concentrations. The unprocessed suspension data in the p-in/p-out polarization configuration reveal the essential angular pattern. The signal falls off towards zero in the forward scattering direction and exhibits oscillations at larger scattering angles. The raw data also suggest that there exists an incoherent contribution to the 2ω signal from the pure MG solution. Observations of MG-only solutions are shown in Fig. 2, also for the p-in/p-out scattering configuration. A large forward scattering signal falls off rapidly with increasing scattering angle. This 2ω signal is the two-photon excited fluorescence of MG [6,19]. The inset exhibits our measurements of this two-photon excitation fluorescence spectrum. The large signal in the forward direction arises because this configuration is sensitive to the largest scattering volume. The excitation wavelength and

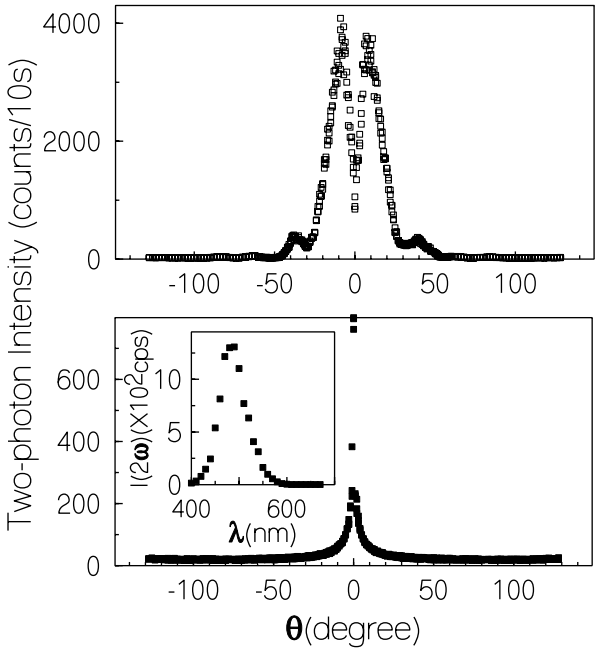

FIG. 2. Raw 2ω light scattering intensity angular profile for $D = 980$ nm suspension (top) and for pure MG solution (bottom) in the p-in/p-out configuration. Inset: two-photon excitation fluorescence spectrum of MG solution for p-in/p-out.

concentrations we chose maximized the signal-to-noise of our angle-resolved measurements. We measured the background signal in all polarization configurations; the signals had similar angular characteristics but different magnitudes.

As described above, the SHG signals from suspensions of colloidal particles in MG solution contain contributions from two sources: bulk MG in solution and adsorbed MG on the particle surfaces. We write the total electric field at 2ω, $\mathbf{E}_{\text{tot}}(2\omega, r, \theta)$, as a sum of the fields from these sources, i.e., $\mathbf{E}_{\text{tot}}(2\omega, r, \theta) = \mathbf{E}_s(2\omega, r, \theta) + \mathbf{E}_{\text{bulk}}(2\omega, r, \theta)$. These two contributions are uncorrelated. For example, the particle-induced electric field, $\mathbf{E}_s$, depends on the positions of all particles, and these positions vary randomly. The particle-induced time-averaged signal intensity, $I_s(2\omega, r, \theta)$, is obtained from the total signal intensity $I_{\text{tot}}(2\omega, r, \theta)$ less the background fluorescence intensity, $I_{\text{bulk}}(2\omega, r, \theta)$, i.e., $I_s(2\omega, r, \theta) = I_{\text{tot}}(2\omega, r, \theta) - I_{\text{bulk}}(2\omega, r, \theta)$. All data exhibited herein are obtained by subtracting background fluorescent intensity in the appropriate polarization configuration from the total intensity.

In Figs. 3 and 4 we present angle-resolved observations. In Fig. 3 we fix the particle size at 700 nm, and explore the effects of polarization configuration. The configurations with p-out have similar profiles with major features confined to $\theta < 50°$, while those with s-out (only p-in/s-out shown) are flat at our measurement noise floor. The largest experimental errors arise in the forward direction, about $\theta = 0°$, where the p-out signals fall to zero and where the background signal is a maximum. Nevertheless, the angular pattern is distinct, and differs qualitatively

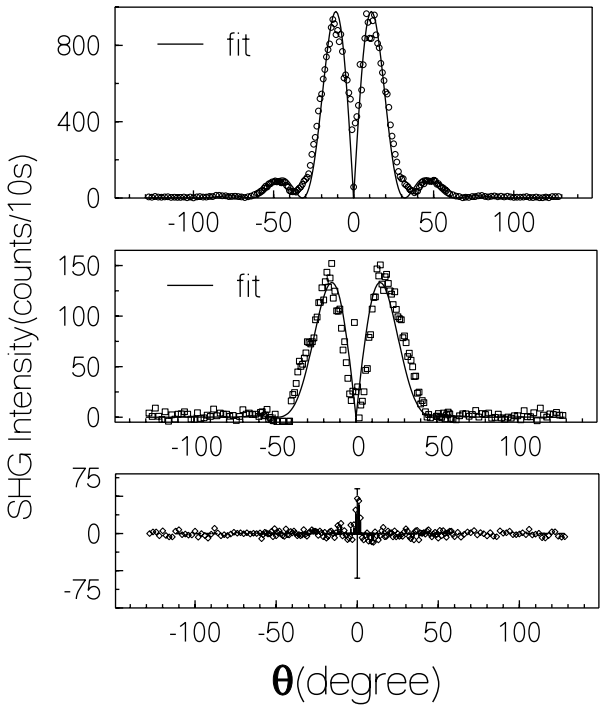

FIG. 3. Extracted SHG scattering angular profile for 700 nm diameter particle. Top: p-in/p-out; middle: s-in/p-out; bottom: p-in/s-out. Also shown is the measurement error at $\theta = 0°$.

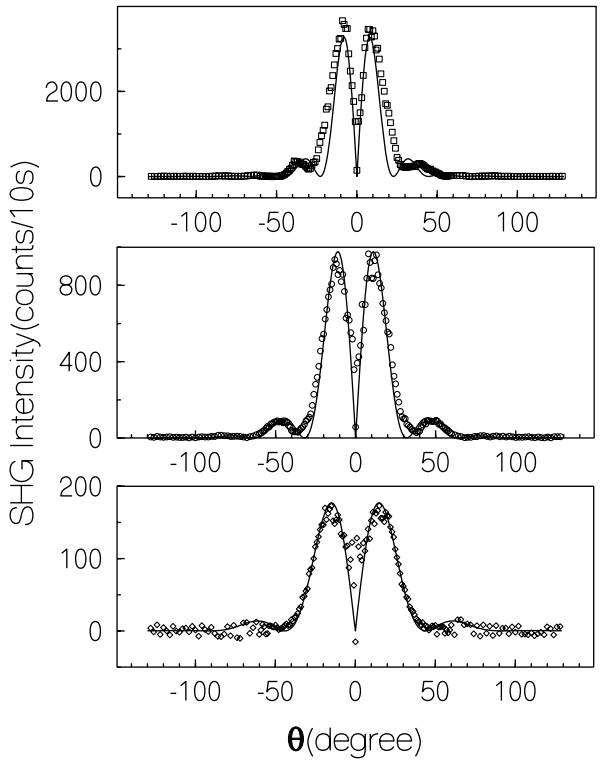

FIG. 4. Extracted SHG scattering angular profile for three different particle diameters in the p-in/p-out configuration. Top: 980 nm; middle: 700 nm; bottom: 510 nm. The lines are fits to the RGD model.

from the linear optical case. The lines represent best fits to the data by using a simple theory discussed below. In Fig. 4 we compare the effects of particle size in a fixed, p-in/p-out, polarization configuration. The signal is larger with increasing particle size, but the angular profiles are similar. A closer examination reveals that the maxima occur at slightly different angles, shifting to larger angles for smaller diameter particles.

We next describe a simple theoretical model to understand the angular patterns of Figs. 3 and 4. The basis of our analysis is the Rayleigh-Gans-Debye approximation for light scattering. The RGD model is applicable when the particle scattering strength is small and when scattering is peaked in the forward direction [2]. In our case, the index mismatch between particles and background fluid is only 20%, and substantive scattering occurs for angles less than $\sim 50°$.

We use the standard Green's function method to compute the scattered field from one sphere. Our signal is an *incoherent sum* of the single-sphere solution:

$$\mathbf{E}_{2\omega}(\mathbf{r}) = \frac{(2\omega)^2}{c^2} \int d^3\mathbf{r}' \, \frac{e^{ik_{2\omega}|\mathbf{r}-\mathbf{r}'|}}{|\mathbf{r} - \mathbf{r}'|} \, \mathbf{P}_{2\omega}^{\mathrm{NL}}(\mathbf{r}'), \quad (1)$$

where $k_{2\omega}^2 = \frac{(2\omega)^2}{c^2}\epsilon(2\omega)$, ϵ is the particle dielectric constant, and $\mathbf{P}_{2\omega}^{\mathrm{NL}}(\mathbf{r})$ is the nonlinear source polarization induced by the input fundamental light. $\mathbf{P}_{2\omega}^{\mathrm{NL}}$ depends on the input beam parameters and the particle properties. To obtain $\mathbf{P}_{2\omega}^{\mathrm{NL}}$, we use the RGD approximation which sets the field inside the particle equal to the field of the input beam. Our coordinate system puts the particle center at the origin and takes the input fundamental beam to propagate along the z direction, with measurements in the xz plane. θ is defined as the angle between the z axis and observation direction. We assume that MG molecules adsorbed on PS surfaces are oriented to point radially outward [6], and that these surface adsorbates are the dominant contribution to $P_{2\omega}^{\mathrm{NL}}$. The molecule's hyperpolarizability is assumed to be zero, except along this radial direction; this hyperpolarizability is denoted $\alpha^{(2)}$, with all other elements of $\alpha^{(2)}$ set to zero.

The substitution and integration of the two forms of $\mathbf{P}_{2\omega}^{\mathrm{NL}}(\mathbf{r})$ into Eq. (1) gives simple solutions for the s-in/p-out and the p-in/p-out cases:

$$\mathbf{E}_{2\omega}^{sp}(\mathbf{r}) \propto \alpha^{(2)} \, \frac{R}{q} \, F_s(\theta) \left(-\sin\frac{\theta}{2} \, \hat{e}_{\parallel} + \cos\frac{\theta}{2} \, \hat{e}_{\perp} \right), \quad (2)$$

$$\mathbf{E}_{2\omega}^{pp}(\mathbf{r}) \propto \alpha^{(2)} \, \frac{R}{q} \left\{ \sin\frac{\theta}{2} \left[F_s(\theta) \left(1 + \cos^2\frac{\theta}{2} \right) - 2F_p(\theta) \cos^2\frac{\theta}{2} \right] \hat{e}_{\parallel} + \cos\frac{\theta}{2} \left[F_s(\theta) \sin^2\frac{\theta}{2} + 2F_p(\theta) \cos^2\frac{\theta}{2} \right] \hat{e}_{\perp} \right\}. \quad (3)$$

Here $\hat{e}_{\parallel}$ and $\hat{e}_{\perp}$ are unit vectors in the longitudinal and transverse directions, respectively, at the observation point. R is the particle radius and $\mathbf{q}$ is the nonlinear scattering vector, $|\mathbf{q}| = 2k_{2\omega}\sin\frac{\theta}{2}$. $F_s(\theta)$ and $F_p(\theta)$ are standard form factors [20] which account for the particle diameter dependence of the scattering. Since we detect the transverse part of the field, we need only retain the transverse part of the solution. The s-out signals are identically zero for all scattering angles in the xz plane. The suppression of s-polarized scattering light agrees with our observations.

We fit the angular intensity profile (solid lines in Figs. 3 and 4) for the p-in/p-out and s-in/p-out cases by using the intensity derived from the transverse part of Eqs. (2) and (3). The overall intensity amplitudes were treated as fitting parameters. There is some deviation at larger scattering angles. As expected, the deviations are larger for larger particles. However, the RGD model fits fairly well, and should prove a helpful approximation in the analysis of future experiments. The good quality fits also corroborate our assumptions about the hyperpolarizability of the adsorbed molecules.

To summarize, we have measured the SHG light scattering angular profile from colloids for the first time, and we have shown how to understand the measurements using a rather simple Rayleigh-Gans-Debye–based theory for SHG light scattering valid for Mie particles. Our results reveal that SHG light scattering in this common experimental scenario is strongly polarization dependent, with little forward scattering and zero s-polarized output. In the future it should be possible to use the angular profiles to discriminate the contributions of particle nonlinear effects from bulk nonlinear effects, and to more quantitatively characterize the particle surfaces.

We gratefully acknowledge NSF support through DMR-97-01657 and DMR-99-71226 and our MRSEC, DMR-00-79909. We thank H. Wang for experimental discussions, T. F. Heinz for sharing theoretical work, and M. Islam, K. H. Lin, and J. Zhang for help characterizing particles.

[1] C. F. Bohren and D. R. Huffman, *Absorption and Scattering of Light by Small Particles* (Wiley, New York, 1983).

[2] M. Kerker, *The Scattering of Light and Other Electromagnetic Radiation* (Academic, New York, 1969).

[3] S. Qian and R. K. Chang, Phys. Rev. Lett. **56**, 926 (1986).

[4] S. C. Hill, D. H. Leach, and R. K. Chang, J. Opt. Soc. Am. B **10**, 16 (1993).

[5] J. Martorell, R. Vilaseca, and R. Corbalán, in *Quantum Electronics and Laser Science Conference* (Optical Society of America, Washington, DC, 1995), Vol. 16, p. 32.

[6] H. Wang, E. C. Y. Yan, E. Borguet, and K. B. Eisenthal, Chem. Phys. Lett. **259**, 15 (1996).

[7] J. I. Dadap, J. Shan, K. B. Eisenthal, and T. F. Heinz, Phys. Rev. Lett. **83**, 4045 (1999).

[8] J. M. Hartings, A. Poon, X. Pu, R. K. Chang, and T. M. Leslie, Chem. Phys. Lett. **281**, 389 (1997).

[9] J. Martorell, R. Vilaseca, and R. Corbalán, Phys. Rev. A **55**, 4520 (1997).

[10] H. Wang, E. C. Y. Yan, Y. Liu, and K. B. Eisenthal, J. Phys. Chem. B **102**, 4446 (1998).

[11] E. C. Y. Yan, Y. Liu, and K. B. Eisenthal, J. Phys. Chem. B **102**, 6331 (1998).

[12] C. S. Yang, H. W. Tom, and M. A. Anderson, in *Centennial Meeting Bulletin of The American Physical Society* (American Physical Society, Atlanta, GA, 1999), Vol. 44, p. 1580.

[13] H. Wang, T. Troxler, A.-G. Yeh, and H.-L. Dai, Langmuir **16**, 2475 (2000).

[14] N. Yang, W. E. Angerer, and A. G. Yodh (to be published).

[15] T. F. Heinz, C. K. Chen, D. Ricard, and Y. R. Shen, Phys. Rev. Lett. **48**, 478 (1982).

[16] T. F. Heinz, H. W. K. Tom, and Y. R. Shen, Phys. Rev. A **28**, 1883 (1983).

[17] W. E. Angerer, N. Yang, A. G. Yodh, M. A. Khan, and C. J. Sun, Phys. Rev. B **59**, 2932 (1999).

[18] R. J. Goldacre and J. N. Phillips, J. Chem. Soc. Part III, 1724 (1949).

[19] M. Yoshizawa, K. Suzuki, A. Kubo, and S. Saikan, Chem. Phys. Lett. **290**, 43 (1998).

[20] $F_s(\theta) = \frac{3}{q^3R^3}[(1 - \frac{1}{3}q^2R^2)\sin qR - qR\cos qR]$, $F_p(\theta) = \frac{3}{q^3R^3}[(1 - \frac{1}{2}q^2R^2)\sin qR - (qR - \frac{1}{6}q^3R^3)\cos qR]$. The coefficient choice for the definition of $F_s(\theta)$ and $F_p(\theta)$ are in analog with the linear RGD form factor. R is the particle radius and $\mathbf{q}$ is the nonlinear scattering vector [assuming $2k_{\omega} = k_{2\omega}$].